J Stat Phys (2014) 155:909–931
DOI 10.1007/s10955-014-0977-z

Critical Study of Hierarchical Lattice Renormalization Group in Magnetic Ordered and Quenched Disordered Systems: Ising and Blume–Emery–Griffiths Models

F. Antenucci · A. Crisanti · L. Leuzzi

Received: 9 October 2013 / Accepted: 13 March 2014 / Published online: 28 March 2014

Abstract Renormalization group based on the Migdal–Kadanoff bond removal approach is often considered a simple and valuable tool to understand the critical behavior of complicated statistical mechanical models. In presence of quenched disorder, however, predictions obtained with the Migdal–Kadanoff bond removal approach quite often fail to quantitatively and qualitatively reproduce critical properties obtained in the mean-field approximation or by numerical simulations in finite dimensions. In an attempt to overcome this limitation we analyze the behavior of Ising and Blume–Emery–Griffiths models on more structured hierarchical lattices. We find that, apart from some exceptions, the failure is not limited to Midgal–Kadanoff cells but originates right from the hierarchization of Bravais lattices on small cells, and shows up also when in-cell loops are considered.

Keywords Hierarchical lattice · Renormalization group · Critical behavior · Migdal–Kadanoff · Ferromagnet · Spin-glass · Ising model · Blume–Emery–Griffiths model

1 Introduction

In this work we shall investigate the renormalization group (RG) analysis of spin systems with quenched disorder on hierarchical lattices. We will consider both Migdal–Kadanoff (MK) as well as more complex hierarchical lattices and we will study the critical behavior of systems with magnetic interactions in presence of random fields and random exchange interactions.

F. Antenucci · A. Crisanti · L. Leuzzi (✉)
Dipartimento di Fisica, Università Sapienza, P.le Aldo Moro 2, 00185 Rome, Italy
e-mail: luca.leuzzi@cnr.it

F. Antenucci · L. Leuzzi
IPCF-CNR, UOS Roma Kerberos, P.le Aldo Moro 2, 00185 Rome, Italy

A. Crisanti
ISC-CNR, UOS Sapienza, P.le Aldo Moro 2, 00185 Rome, Italy

Our main aim is to investigate whether hierarchical cells more complicated than MK ones and more similar to the local structure of short-range Bravais lattices can reproduce features of ferromagnets and spin-glasses so far unobserved in Real Space Renormalization Group (RSRG) studies with MK lattices. In order to obtain a more general comprehension of the effect of bond moving we will provide estimates for critical quantities on several hierarchical lattices with different topology and compare them to known analytic and numerical results, when available.

Particular attention will be devoted to the spin-glass phase. Understanding the nature of the low temperature phase of spin-glasses in finite dimensional systems has turned out to be an extremely difficult task. Since the resolution of the mean-field approximation, valid above the upper critical dimension ($d = 6$), more than thirty years have passed without a final word about the possible generalization of mean-field properties of spin-glasses to finite dimensional cases. The mean-field, else called Replica Symmetry Breaking (RSB) theory [1,2] involves a very interesting solution for the spin-glass phase and its critical properties, rich of physical (and mathematical) implications, and has been fundamental in solving very diverse problems both in physics and in other disciplines [3–5]. Because of its complicated structure, to overcome technical (maybe also conceptual) obstacles hindering the "portability" of RSB theory predictions to short-range systems on Bravais lattice in $d < 6$ is a rather big challenge in theoretical physics. Indeed, the RSB solution is so complex that non-perturbative effects cannot be taken under control in any perturbative loop-expansion around the upper critical dimension and critical scaling behavior is yet to be understood [6–11]. The main hindrance is the lack of translational invariance for locally frustrated systems with quenched disordered interactions, making the techniques developed for quantum field theory and successfully exported to statistical mechanical problems [12,13], e.g., the Ising model critical exponents, inapplicable.

For what concerns Kadanoff original approach in real space [14,15], a proper extension of RG techniques to disordered and locally frustrated systems is still on its way. The generalization of classic RSRG methods on Bravais lattices to disordered interaction, such as the ones proposed for Ising spin models in the seventies [16,17], has led to controversial results. On the one hand, by means of a cumulant expansion approach, evidence for a spin-glass phase is yielded in dimension two [18,19], lower than the lower critical dimension on the Bravais lattice: $d = 2.5$ [20–22]. On the other hand, the renormalization through block transformation on spin clusters does not yield any spin-glass fixed point even in dimension three [18].

The only results have been achieved using "realizable" approximations, namely those that are the exact solution of some alternative problem. The first and most famous example is that of the classic "bond-moving" approximate MK transformation, that when applied to Ising models on Bravais lattices provides the exact solution for an Ising model on a very different lattice [23], known as "hierarchical" lattices [24]. Note that, because of the "bond-moving" procedure, the hierarchical lattices corresponding to MK transformation (MK lattices in the following) have basically a 1D topology, as, e.g., the "necklace" lattice in Fig. 1.

Therefore, most of the RSRG studies have been concentrating on hierarchical lattices for which, in the ordered cases, the RG flow is indeed exact (no truncation required). The study of these systems has brought to important results, cf., e.g., Refs. [23,25–27] and references therein.

However, MK lattices fail to represent short-range spin-glasses on Bravais lattices also in the mean-field approximation and are, thus, strongly limited in probing the actual nature of the spin-glass phase [28,29]. For what concerns perturbative disorder in ferromagnetic systems, it has been found that the Nishimori conjecture does not provide the exact value of

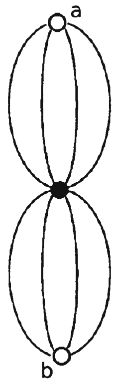

Fig. 1 Necklace MK lattice. It has $b = 2$ and fractal dimension $d = 3$

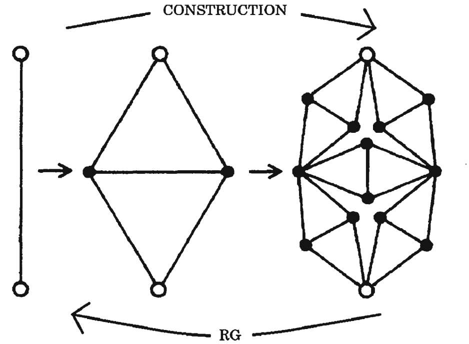

Fig. 2 Construction of the diamond, also called 2D WB HL. The lattice has fractal dimension $d = \log 5/\log 2 = 2.3219\ldots$

the multicritical point coordinate [26,30]. Recently Ohzeki, Nishimori and Berker [26,31] have put forward an improved conjecture for models on hierarchical lattices finding in many cases a noteworthy recovery of the critical properties.

The lack of translational invariance on hierarchical lattices is supposed to make peculiarly difficult the study of first order transitions. For pure systems, while the expected first order transition is obtained in some model (see for example [32,33]), there are relevant cases in which the transition is missing on MK lattices [34,35]. For disordered systems it is known that MK lattices fail to locate the first order transition in the random Blume–Emery–Griffiths model [33], predicted by both mean-field theory [36] and numerical simulations in finite dimension [37], nor the expected re-entrance in the phase diagram [33,36,37].

Our aim is to study whether, and which of the, above mentioned differences are consequence of the bond moving procedure at the basis of the MK RG analysis, and if these are partially, or completely, removed on more structured lattices. We will thus compare the RSRG analysis of the critical behavior of well known statistical mechanical models with quenched field and bond randomness on both MK lattices and the more structured "folded hierarchical lattices", as we will call them.

The latter family consists of hierarchical lattices obtained by applying the two root reduction directly to the Bravais lattice [35] (see Figs. 2, 3, 5, 6, 9), without the bond moving specific of the MK transformation. So the final lattice has no longer just a 1D topology, but retains, in a small scale, the basic topology of the original lattice. So, unlike the MK family, in this case the original lattice is continuously reconstructed in the limit in which the length b of the basic cell goes to infinity: the original lattice is a folded hierarchical lattice with an infinite basic cell.

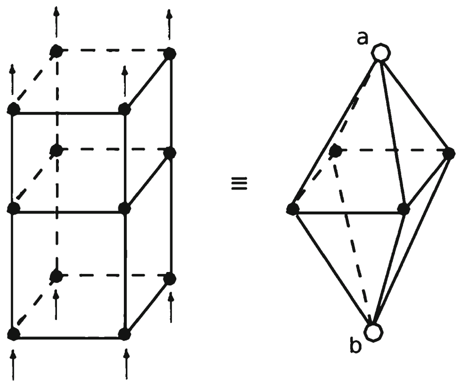

Fig. 3 3D WB HL obtained from a cubic lattice by grouping together the *incoming* and *outcoming* spins denoted by the *arrows*. The HL has $b = 2$ and fractal dimension $d = \log 12/\log 2 = 3.585\ldots$

In the following, we will first critically revisit, in each model case, the analysis on hierarchical lattices carried out in the literature. We will, then, compare those results to the outcome of our studies on more complex lattices in the family of folded cells.

The paper is organized as follows: in Sect. 2 we recall the implementation of the RSRG in the ferromagnetic Ising model. In Sect. 2.1 we extend the RSRG in presence of generic quenched disorder. In Sect. 2.2, we investigate the Random Field Ising model (RFIM) and in Sects. 2.3 and 2.4 the Ising spin-glass, respectively below and above the lower critical dimension. We compare known and new estimates of critical parameters and discuss how they comply to known statistical mechanical criteria in presence of disorder. In Sect. 3 we consider the Blume–Emery–Griffiths model in dimension $d \geq 3$. Our analysis shows a re-entrance in the phase diagram for strong disorder, absent on MK lattices [33] but found in the mean-field approximation [38] and in numerical simulations on 3D cubic lattices [37,39,40].

2 Hierarchical Renormalization: Ising Model

The RSRG approach, approximated on realistic Bravais lattices, becomes exact on Hierarchical Lattices (HL) [14,23,24,35,41]. These lattices are constructed by carrying successive similar operations, that is, one moves from one hierarchical level to the next one by replacing each bond by a well-defined unit cells. See, for example, Fig. 1 for a MK lattice or Fig. 2 for the diamond lattice. The RSRG procedure works the reverse way, i.e., one performs a decimation of the internal sites of a given cell, leading to renormalized interactions among the survived sites, and hence moves up of one hierarchical level.

Since the decimation procedure may produce additional interactions the starting Hamiltonian of the Ising model is:

$$-\beta\mathcal{H}(\boldsymbol{s}) = \sum_{\langle ij\rangle}\left[J_{ij}s_i s_j + h_{ij}\frac{s_i+s_j}{2} + h^{\dagger}_{ij}\frac{s_i-s_j}{2}\right] \tag{1}$$

where $s_i = \pm 1$ and $\langle ij\rangle$ indicates a sum over nearest-neighbor pairs. We use reduced parameters in which the temperature is absorbed into the couplings.

Decimating the inner sites $\{s\} = \{s \in \mathcal{C}_{ab} \mid s_a, s_b\}$ of the basic cell $\mathcal{C}_{ab}$ of the hierarchical lattice with external sites s_a and s_b, while imposing the conservation of the partition function of the cell

$$Z_{\mathcal{C}_{ab}} \equiv x_{s_a s_b} = \sum_{\{s\}} e^{-\beta\mathcal{H}(s)}, \tag{2}$$

yields the RG equations:

$$J_R = \frac{1}{4}\log\left(\frac{x_{++}x_{--}}{x_{+-}x_{-+}}\right), \qquad h_R = \frac{1}{2}\log\left(\frac{x_{++}}{x_{--}}\right), \qquad h_R^\dagger = \frac{1}{2}\log\left(\frac{x_{+-}}{x_{-+}}\right). \tag{3}$$

The partition sums $x_{s_a s_b}$, also called edge Boltzmann factors of the cell, are the weights of the cell for fixed external spins s_a and s_b. The sum in Eq. (2) runs over all inner or free spins of the cell $\mathcal{C}_{ab}$. Note as when the external field is missing $h = h^\dagger = 0$ and $\mathcal{H}(s) = \mathcal{H}(-s)$, which implies $h_R = h_R^\dagger = 0$.

The fixed points of the RG equations identify the phases of the model and, in the pure case, the critical exponents are obtained from the eigenvalues of the stability matrix of the fixed point [42]. If at the fixed point $h = h^\dagger = 0$ then the stability matrix is diagonal with scaling exponents $y_{T,h} = \log_b \lambda_{T,h}$, where $\lambda_T = \partial_J J_R$ and $\lambda_h = \partial_h h_R$ and b the length of the cell in lattice spacings, i.e., the scaling factor in the decimation procedure. From these one obtains the critical exponents $\nu = 1/y_T$ and $\eta = d + 2 - 2\,y_h$, while the others follow from the usual scaling relations for the pure Ising model [42].

2.1 Hierarchical Renormalization in Presence of Quenched Disorder

In disordered systems one has to consider the evolution of the whole coupling probability distribution $P(\mathcal{K})$ [43,44], rather than that of a single coupling configuration $\mathcal{K} : \mathcal{K}^R = \mathcal{R}(\mathcal{K})$. The RG equation then becomes

$$P_R(\mathcal{K}^R) = \int d\mathcal{K}\, P(\mathcal{K})\, \delta\big[\mathcal{K}^R - \mathcal{R}(\mathcal{K})\big] \tag{4}$$

Practically the RSRG scheme is accomplished by representing the probability distribution $P(\mathcal{K})$ by a pool of M real numbers [45]. The process then starts by creating a pool of M coupling constants generated using the initial probability distribution. A RSRG iteration consists in M operations in which one randomly picks a set of b^d couplings from the pool and generate one renormalized coupling. Following this procedure, one creates a new pool of size M representing the renormalized probability distribution form which the moments can be evaluated. We have used pools up to $M = 10^6$, large enough to guarantee statistically stable results.

The evolution of the moments of $P(\mathcal{K})$ are of particular interest for the identification of the phases. In the Ising models with quenched disorder, denoting by $\mu_J = [J_{ij}]$ the average of the couplings and by $\sigma_J^2 = [(\delta J_{ij})^2]$ its variance, the Paramagnetic (PM), Ferromagnetic (FM), and Spin Glass (SG) phases, are identified by the attractors

$$\begin{array}{lll} \mu_J \to 0; & \sigma_J \to 0; & \text{PM;} \\ \mu_J \to \infty; & \sigma_J \to \infty \quad (\mu_J/\sigma_J \to \infty)\,; & \text{FM;} \\ \mu_J \to 0; & \sigma_J \to \infty; & \text{SG.} \end{array}$$

To reduce the finite pool size effects, the procedure is repeated for N_s different pools, typically from 10 to 20. This is especially relevant near a critical point, where due to finite pool size effects, different pools can flow towards different attractors. We have adopted the convention that a phase is identified if at least 80 % of the pools flow into the same attractor, and this fixes the error on the location of critical points.

Table 1 Critical value of J and h_0 for the RFIM on the necklace MK lattice, Fig. 1, and WB lattice, Fig. 3, with bimodal or Gaussian distribution of random fields

Lattice	h_0	h_0/J
Bimod. MK	0.942(4)	0.876(3)
Gauss MK	0.934(5)	0.869(4)
Bimod. WB	0.460(2)	0.443(5)
Gauss WB	0.456(3)	0.448(4)

In presence of disorder it is difficult to give an analytical prescription for computing the critical exponents. These can be estimated by following the RG flow close to the unstable fixed point. We will discuss this procedure in detail.

2.2 Random Field Ising Model

In this section we discuss the RSRG study of the RFIM and compare the results on the necklace MK lattice with fractal dimension $d = 3$ of Fig. 1 [46] with those on the Wheatstone–Bridge (WB) hierarchical lattice with fractal dimension $d = 3.585\ldots$ of Fig. 3.[1]

The initial probability distribution $P(\mathcal{K})$ of couplings is

$$P(J_{ij}, h_{ij}, h^{\dagger}_{ij}) = \delta(J_{ij} - J)\, p(h_{ij})\, \delta\left(h^{\dagger}_{ij}\right) \tag{5}$$

where $p(h_{ij})$ is either a bimodal or a Gaussian distribution:

$$p(h_{ij}) = \begin{cases} \frac{1}{2}\left[\delta(h_{ij} - h_0) + \delta(h_{ij} + h_0)\right], \\ \frac{1}{\sqrt{2\pi h_0^2}} \exp\left(-h_{ij}^2/2h_0^2\right). \end{cases} \tag{6}$$

$P(\mathcal{K})$ is an even function of h_{ij} and $h^{\dagger}_{ij}$. This symmetry is preserved under the RSRG transformation. To enforce it on a finite pools we symmetrize the pool by adding for each renormalized interactions $(J_{ij}, h_{ij}, h^{\dagger}_{ij})$ the symmetric one $(J_{ij}, -h_{ij}, -h^{\dagger}_{ij})$. This doubles the pool size but reduces the bias on the RSRG flow, especially with small pool sizes.

The critical behavior of the RFIM is controlled by a zero-temperature fixed point where both μ_J, the coupling average, and σ_h, the field standard deviation, flow to infinity. The critical point separates the high temperature phase, $\sigma_h\,/\,\mu_J \to \infty$, from the low temperature phase, $\sigma_h\,/\,\mu_J \to 0$. The zero-temperature fixed point can be identified by searching for the values of J and h_0 for which the ratio $\sigma_h\,/\,\mu_J$ approaches a finite, non-zero, value. The numerical critical values are reported in Table 1, whereas the fixed point probability distribution is shown in Fig. 4.

The zero-temperature fixed point is characterized by three independent exponents: the coupling probability distribution scaling exponent y, the magnetic field scaling exponent y_h and the thermal scaling exponent y_T. From the scaling exponents one has the critical exponents $\nu = 1/y_T$, $\alpha = 2 - (d - y)\nu$ and $\beta = (d - y_h)\nu$, and the others follow from the scaling relations [49]. The scaling exponents can be estimated by using the following procedure [46].

[1] Previous results [47] on this lattice suffers from some inconsistency, as discussed in Ref. [48].

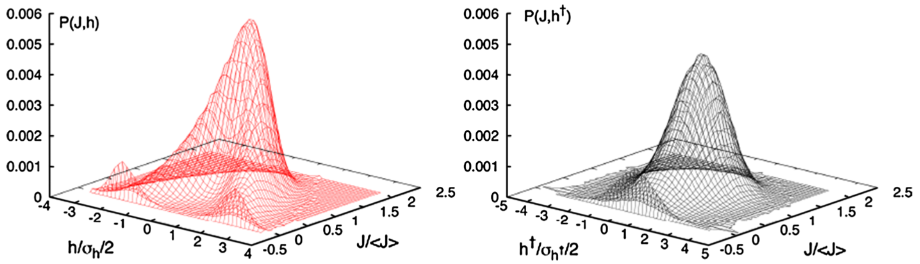

Fig. 4 Zero-temperature fixed point probability distribution for RFIM on 3D WB lattice with bimodal initial distribution: $P(J, h)$ (*left*) and $P(J, h^\dagger)$ (*right*). The Gaussian case is similar. The fixed point probability distribution is invariant under an arbitrary scale factor. In the plots $\sigma_h/\mu_J = h_0/J$

2.2.1 Distribution Scaling Exponent

The exponent y measures the growth of the width of the couplings probability distribution under renormalization. The fixed point probability distribution P^* is invariant under an arbitrary scale factor. Therefore to estimate y we start on the phase boundary and evaluate the rescaling factor $\lambda = \sigma_{h_R}/\sigma_h = \mu_{J_R}/\mu_J$ which measure the growth of the width along the renormalization flow. To balance the drift of the RG flow away from the (unstable) critical surface, at each renormalization step the probability is moved back by shifting the couplings by $0.8 \times (\mu - \mu_J)$ with $\mu = \sigma_h/(h_0/J)$. The shift is usually of the order of 0.1 % for each coupling.

The exponent y is estimated as

$$y = \log_b \overline{\lambda}, \tag{7}$$

where the overbar denotes average along the RG flow, 10 RSRG steps in our case. The estimated values are given in Table 2. In all cases $y \leq d/2$, the upper bound provided by Berker and McKay [50].

2.2.2 Field Scaling Exponent

The exponent y_h measures the growth of an infinitesimal homogeneous symmetry-breaking external field h under RG, and is given by

$$y_h = \log_b \left[\frac{\partial h_R}{\partial h} \right]_{P*} \tag{8}$$

where the average is taken with the zero-temperature fixed point probability distribution P^*. The values are reported in Table 2. In all cases the value is smaller than the fractal dimension, 3 for MK and 3.585 . . . for WB, and the magnetization is continuous at the transition.

2.2.3 Thermal Scaling Exponent

The scaling exponent y_T describes how the RG flow leaves the critical surface, and can be evaluated by comparing two close RG flows. The pool representing the fixed point distribution P^* is then duplicated, and the copy is slightly perturbed by shifting all couplings J_{ij} by the small amount $\delta = 10^{-4} J$. The two copies are simultaneously transformed, with the original kept close to the critical surface as done for the computation of y, while the second is left

Table 2 Scaling exponents of RFIM on the necklace MK lattice of Fig. 1 and the WB lattice of Fig. 3

Lattice	y	y_h	y_T
Bimod. MK	1.491(3)	2.991(1)	0.45(23)
Bimod. MK [51]	1.4916(3)	2.9911(2)	0.445(2)
Gauss MK	1.486(3)	2.990(1)	0.44(20)
Bimod. WB	1.788(2)	3.575(1)	0.69(35)
Gauss WB	1.787(2)	3.576(1)	0.68(31)
3D sim. [52]	1.49(3)	2.988(4)	0.73(5)
4D sim. [53]	1.779(4)	3.827(1)	1.280(2)

The scaling exponents on the MK lattice with bimodal field are in agreement with those of Ref. [46]. The more accurate values of Ref. [51] are obtained using the histograms representation for the interactions probability distribution, feasible only on MK cells. The last two rows refer to simulations on 3D and 4D regular lattices with bimodal distributed fields

free to depart from it. At each step the difference t between the values of σ_h/μ_J from the two pools are recorded. The scaling exponent y_T is evaluated as

$$y_T = \log_b \overline{\left(\frac{t_{n+1}}{t_n}\right)}, \tag{9}$$

where t_n is the difference after n RSRG steps, and the average is along the RG flow. [2] Typically n ranges from 3 to 9, so that perturbed pool is not too far from the critical surface, while $M \gtrsim 10^5$ to have a stable results. The values are reported in Table 2.

The exponents y and y_h depend strongly on the fractal dimension d of the lattice. The values for the MK lattice, $d = 3$, are in good agreement with the results of numerical simulations of the RFIM with bimodal field distribution on the cubic lattice, while those on WB lattice, $d = 3.585\ldots$, are closer to the results of simulations on the 4D lattice.

The value of y_T for the WB hierarchical lattice is larger than that for the MK lattice, in agreement with the trend seen in the numerical simulations.

The values for the Gaussian and bimodal case are compatible with each other, indicating that they belong to the same universality class.

2.3 Random Bond Ising Model in $d \leq 2.5$

In this section we consider the Ising model, Eq. (1), with random $\pm J$,

$$P(J_{ij}, h_{ij}, h^\dagger_{ij}) = \left[p\delta(J_{ij} - J) + (1-p)\delta(J_{ij} + J)\right] \delta\big(h_{ij}\big)\delta\big(h^\dagger_{ij}\big), \tag{10}$$

with $p \in [0, 1]$, on hierarchical lattices mimicking the topology of the 2D square lattice. The presence of bond disorder, absent in the RFIM, needs a finer treatment of the bond structure in the RG analysis, and is one of the main reasons of moving from MK lattice to more structured HL. We shall consider the *folded square* (FS) HL in Fig. 5 with $b = 3$ proposed by Nobre [30], and its extension to $b = 5$ shown in Fig. 6.

On a regular lattice for p low enough there exists an antiferromagnetic (AFM) phase. On HL the AFM order is preserved under RSRG only if the rescaling factor b is odd and the RG equations are antisymmetric for $J \to -J$. The phase diagram is then symmetric for

[2] The argument of the logarithm is always positive because the variance can either shrink or increase but does not oscillate between different RSRG steps.

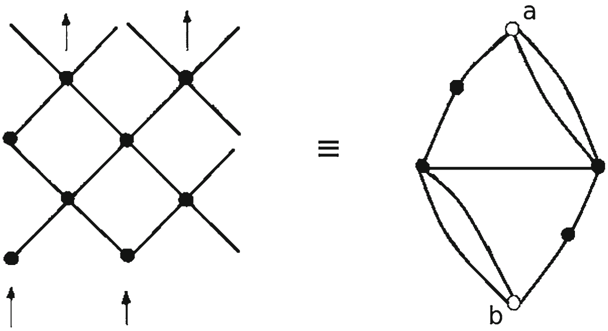

Fig. 5 *Left* square lattice cells. *Right* $b = 3$ *folded square* HL with two roots (*empty dots*). The *outcoming* and *incoming* sites, indicated by the *arrows*, are collapsed and replaced by the root sites a and b. The 4 inner sites of the square cell become the inner sites (*filled dots*) of the HL. This construction gives a self-dual lattice with fractal dimension $d = \ln 9/\ln 3 = 2$

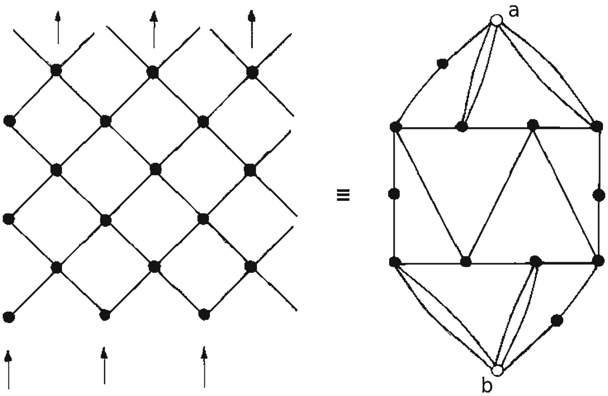

Fig. 6 *Left* square lattice cells. *Right* $b = 5$ *folded square* HL with two roots (*empty dots*). For the construction see Fig. 5. The lattice has fractal dimension $d = \ln 25/\ln 5 = 2$

$p \leftrightarrow (1-p)$, and hence under the exchange of the FM and AFM phases. The phase diagram of the 2D model obtained with the $b = 5$ FS HL is shown in Fig. 7.

The pure FM fixed point, $p = 1$, occurs at the critical temperature $T_c = J_c^{-1} = 2.269185(1)$, in quite good agreement with the Onsager exact result $T_c = 2/\log(1+\sqrt{2}) = 2.269185\ldots$ This result, found also with the $b = 3$ FS HL [30] and the WB HL with $d = 2.32$ [27], follows from the duality properties of the unit cells [35].

The scaling exponents of the $p = 1$ fixed point can be estimated as discussed in Sect. 2. We find $y_T = 0.7303(1)$ and $y_h = 0.8518(1)$ for the $b = 3$ FS and $y_T = 0.7589(1)$ and $y_h = 1.059(1)$ for the $b = 5$ FS, either way, not consistent with those from the Onsager solution: $y_T = 1$ and $y_h = 1.875$. The critical exponents are reported in Table 3.

For both FS HL we found $\alpha < 0$. According to the widely accepted form of the Harris criterion [54,55] the disorder in ferromagnetic systems is irrelevant if the exponent α of the pure system is negative. This agrees with the direct analysis of the RG flow which reveals no other fixed points besides the pure FM $p = 1$ one, and hence no different universality classes in presence of disorder. The typical evolution on the critical surface of the coupling probability distribution is shown in Fig. 8. Though it is known that this criterion can fail on

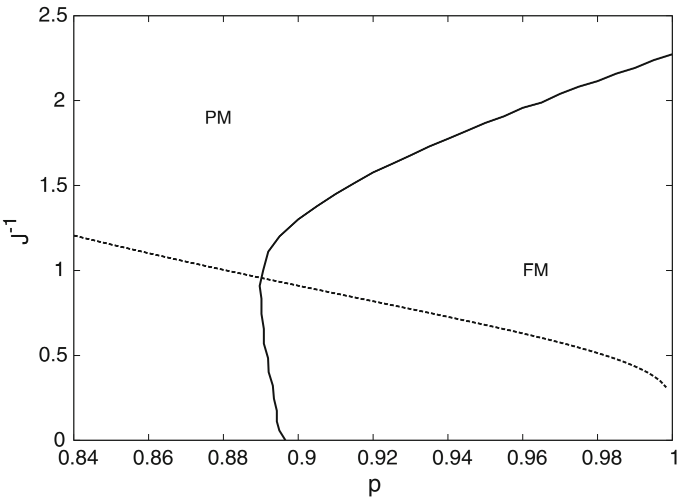

Fig. 7 $(p, T = J^{-1})$ phase diagram of the 2D $\pm J$ Random Bond Ising model on the $b = 5$ FS HL. The phase diagram is symmetric under $p \to 1 - p$ and only the PM/FM region is shown. The *dashed line* is the Nishimori line, see text

Table 3 Critical exponent of the pure FM critical point of the 2D $\pm J$ Random Bond Ising model on the folded square HL

	$b = 3$ folded square	$b = 5$ folded square	Exact
α	−0.7385(1)	−0.6353(1)	0
β	1.572(1)	1.240(1)	0.125
γ	−0.4057(1)	0.1558(1)	1.75
δ	0.7419(1)	1.126(1)	15
ν	1.369(1)	1.318(1)	1
η	2.296(1)	1.882(1)	0.25

HL if the bonds in the cell are not all equivalent [44,56–60], the Harris criterion appears satisfied for the $b = 3$ and $b = 5$ FS HL.

Another quantity used to infer the relevance of the disorder is the slope of the critical line at $p = 1$ [54]:

$$s \equiv \frac{1}{T_c(p)} \frac{dT_c(p)}{dp}\bigg|_{p=1}. \tag{11}$$

For the 2D $\pm J$ Random Bond Ising model the Domany's perturbative approach yields $s = 2\sqrt{2}/[\ln(\sqrt{2}+1)] = 3.209\ldots$ [61]. This assumes from the beginning *weak* disorder, i.e., irrelevant disorder and hence no change in the universality class of the PM/FM transition for $p < 1$. Ohzeki and collaborators have suggested [62] that by comparing the value of s one can discriminate whether or not the quenched disorder is a relevant perturbation on self-dual lattices, causing a change in the universality class. For the $b = 3$ FS we obtain $s = 3.30(3)$, compatible with the value of $s = 3.27866$ from duality arguments [62]. For the $b = 5$ FS the estimated value is $s = 3.32(3)$. Either way, the values are different from the Domany's value $s = 3.209\ldots$. According to the arguments of Ref. [62] this would imply that disorder is relevant. We then conclude that if it is true that a slope equal to Domany's value might be

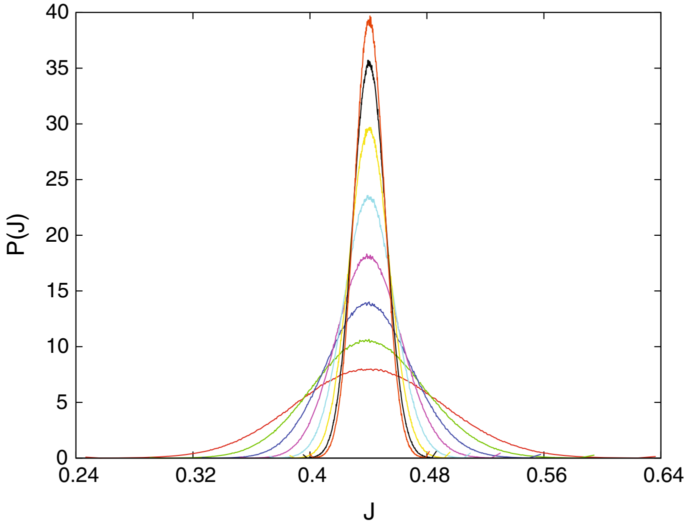

Fig. 8 Evolution of the coupling distribution on the critical surface. The width quickly decreases, the distribution tends to a delta function and the disorder disappears. In figure steps from 4 to 11 and $p = 0.99$

consistent with the irrelevance of disorder, a value different from Domany's value does not necessarily implies the relevance of disorder. The RG approach on the $b = 3$ and $b = 5$ FS HL fails to give a quantitatively exact description of the critical behavior and the numerical discrepancy with the Domany's value can just be a consequence of this.

Even though the 2D Random Bond Ising model does not display an SG phase [63], its study on hierarchical lattices is an excellent test of the Nishimori's conjecture [64–68]. In the 3D model the Nishimori's conjecture identifies the point on the Nishimori line $e^{-2J} = (1-p)/p$ where $H(p_{\rm mc}) = -p\log_2(p_{\rm mc}) - (1-p_{\rm mc})\log_2(1-p_{\rm mc}) = 1/2$ with the multicritical point where the PM, FM and SG phases meet. In the 2D model the SG phase is absent and the point should coincide with an unstable critical point on the PM/FM phase boundary. The Nishimori's conjecture is known to fail on some HL [26,31,69]. We then test it on the FS HL.

From the Nishimori's conjecture the intersection between the PM/FM boundary and the Nishimori line should occur at $p_{\rm mc} \simeq 0.889972$. For the $b = 3$ FS HL the crossing occurs at $T_{\rm mc} = 0.9557(18)$ with $p_{\rm mc} = 0.8903(2)$, leading to $2H(p_N) = 0.998(1)$ [26,30]. For the $b = 5$ FS HL we find

$$T_{\rm mc} = 0.9571(1), \quad p_{\rm mc} = 0.8902(1) \tag{12}$$

with $2H(p_N) = 0.9985(1)$, similar to what found with the $b = 3$ folded square cell. We then conclude that the conjecture also fails on FS HL. Note that the values obtained with the folded square cell agree with the estimate $p_{\rm mc} = 0.8905(5)$ from the transfer matrix approach [70], but are slightly larger than those from the high temperature series expansion, $p_{\rm mc} = 0.886(3)$ [71], and Monte Carlo simulations, $p_{\rm mc} = 0.8872(8)$ [72].

An important feature of the p, T phase diagram, which follows from duality, is the re-entrance of the transition line below the multicritical point, i.e., $p_{T=0} > p_{\rm mc}$. With the $b = 3$ FS one has $p_{T=0} = 0.8951(3)$ [30], while with the $b = 5$ FS the value is $p_{T=0} = 0.8966(2)$, confirming the re-entrance in both cases. These values are consistent with those from the finite

Table 4 Stiffness exponent θ for the 2D Gaussian Random Bond Ising model on different HL

Lattice type	θ
$b = 2$ MK	$-0.270(2)$ [45]
$b = 3$ MK	$-0.278(2)$ [76]
$b = 2$ WB	$-0.290(3)$ [35]
$b = 3$ WB	$-0.298(2)$ [76]
$b = 3$ FS	$-0.275(1)$ [35]
$b = 5$ FS	$-0.2714(2)$
	$-0.291(2)$ [74]
2D square	$-0.287(4)$ [77]
	$-0.284(4)$ [78]

The last tree lines refers to direct numerical simulations

size scaling analysis of the ground state, that leads to $p^{(\rho)}_{T=0} = 0.896(1)$ or $p^{(\theta)}_{T=0} = 0.894(2)$, depending on which exponent is used to characterize the transition [73].

We conclude the analysis of the 2D model with a discussion of the zero temperature stiffness exponent θ. The exponent θ is related to the scaling of the bond probability distribution width σ_J under the RG transformation:

$$\sigma_{J_R}(b) \sim \sigma_J b^{\theta}. \tag{13}$$

A positive (negative) θ means a RG flow that flow towards a strong (weak) couplings fixed point, distinctive of a low temperature SG (high temperature PM) phase. For continuous and symmetric probability distributions $P(J)$ the temperature T appears in the RSRG equations as a dimensionless ratio between couplings, and the scaling (13) implies that the typical size of the "droplets" of aligned spins goes as $L \sim T^{1/\theta}$ [74]. For a phase transition at $T = 0$ this readly leads to the correlation length scaling $\xi \sim T^{-\nu}$ with $\nu = -1/\theta$ [75].

To compare with known results, we have considered the case of a zero-average Gaussian bond distribution, finding $\theta = -0.275(1)$ [$\nu = 3.635(0)$] for the $b = 3$ FS, in agreement with Ref. [76], and $\theta = -0.2714(2)$ [$\nu = 3.684(3)$] for the $b = 5$ FS. The values found for others HL are shown in Table 4. The values for the FS are similar to those found on the MK lattice, whilst the values for the WB lattices are closer to those of the regular 2D lattice.

From the above study we conclude that in passing from $b = 3$ to $b = 5$, and thus increasing the connectivity of the lattice, we obtain in general a slight improvement in the numerical values the critical exponents of the pure fixed point, cfr. Table 3. The values, however, remain far from the exact ones. This rather slow convergence may indicate that the degree of the internal correlation of the FS cell required to correctly describe the critical behavior might be so large to make the single FS cell comparable with a whole real Bravais lattices.

2.4 Random Bond Ising Model in $d > 2.5$

In this section we consider the $\pm J$ Random Bond Ising model on HL mimicking the 3D cubic lattice topology, where the SG phase should be present. To stress this we call the model $\pm J$ Ising SG model. Recently Salmon et al. [27] have obtained accurate phase diagrams for the Ising SG on the WB HL in Figs. 2 and 3, and shown that on these lattices the lower critical dimension of the SG phase is larger than $d = \ln 5/\ln 2 = 2.32\ldots$, cfr. Fig. 2. The fractal dimension of the WB HL in Fig. 3 is $d = 3.585\ldots$, greater than the expected lower critical dimension 2.5 of the SG transition, but also greater than $d = 3$. Quantitative deviations from the 3D cubic lattice might, then, occur.

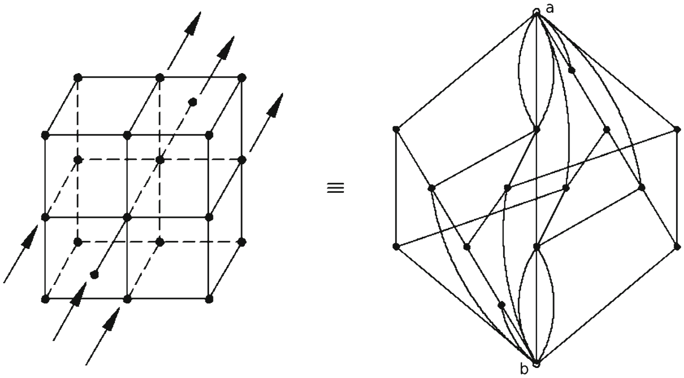

Fig. 9 *Left* cubic cells with $b = 3$. *Right* $b = 3$ *folded cube* HL. The *incoming* and *outcoming* sites, indicated by the *arrows*, are collapsed and replaced by the two root sites a and b (*empty dots*). The other sites of the cubic cell become the inner sites of the hierarchical cell (*filled dots*)

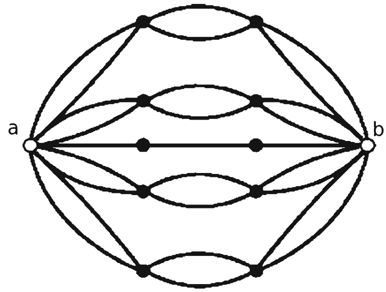

Fig. 10 $b = 3$ MK cell with fractal dimension $d = 3$ [69,79]

We study the model on the Folded Cube (FC) HL shown in Fig. 9. This is the "three-dimensional" extension of the FS lattice of Fig. 5 introduced to study the anisotropic 3D ferromagnetic Potts model [34]. This lattice has a fractal dimension $d = \ln 35/\ln 3 = 3.2362\ldots$, and hence closer to 3 than the WB lattice. Moreover it has $b = 3$ and, unlike the WB, it may retain a possible AFM order. For comparison we also consider the MK lattice in Fig. 10 ($b = 3$ MK) with $b = 3$ and fractal dimension $d = 3$ introduced in Refs. [33,79].

The phase diagram of the $\pm J$ Ising SG model on the $b = 3$ FC HL is shown in Fig. 11. Note the small re-entrance just below the muticritical point, so that by decreasing the temperature one passes from the PM phase to the ordered FM phase, and then to the disordered SG phase. The position of the critical points is reported in Table 5.

The points on the critical PM/FM line (critical surface) flow under RG towards the pure FM fixed point located at $p = 1$. The value $T_c = 5.066(1)$ on the $b = 3$ FC HL is 12 % larger than the estimated value $T_c = 4.5115$ from numerical simulations on the 3D lattice [80]. We note that with the 3D WB the difference increases to 21 % [27], while the best known MK result obtained with the $b = 3$ MK lattice is 19 % larger [79].

The scaling exponents of the FM fixed point on the $b = 3$ FC HL are $y_T = 1.523(1)$ and $y_h = 1.864(1)$. With the 3D WB one has $y_T = 1.149(1)$ and $y_h = 0.9636(1)$, whereas $y_T = 1.460(1)$ and $y_h = 1.613(1)$ on the $b = 3$ MK lattice. In all cases $y_h < d$ and the transition is continuous [81], however none of these agree with the result from numerical simulation on 3D lattice, $y_T = 1.587(1)$ and $y_h = 2.482(1)$ [82], yet the $b = 3$ FC HL gives the closest estimation. The critical exponents are reported in Table 6.

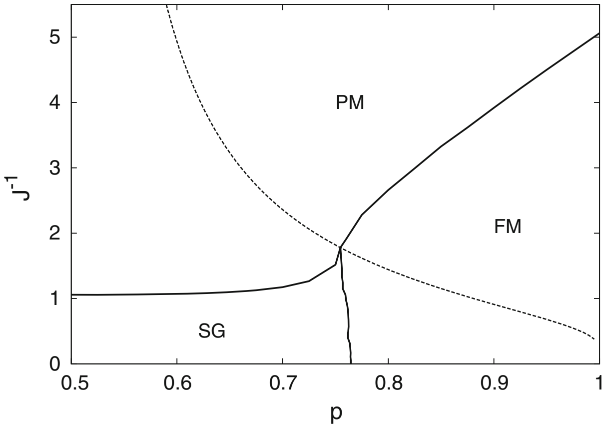

Fig. 11 $(p, T = J^{-1})$ phase diagram of the $\pm J$ Ising SG model on the $b = 3$ FC HL. The *dashed line* is the Nishimori line. The plot is symmetric under $p \to 1 - p$ and only the FM part is shown

Table 5 Critical points of the $\pm J$ Ising SG on various HL

		$b = 3$ FC	3D WB	4D WB [27]	$b = 3$ MK
FM	p	1	1		1
	T	5.066(1)	5.457(1)		5.383(1)
SG	p	0.5	0.5	0.5	0.5
	T	1.072(1)	1.112(2)	2.515(2)	1.136(4)
$T = 0$	p	0.764(2)	0.760(1)	0.667(2)	0.761(1)
	T	0	0	0	0
Muticritical	p	0.7547(3)	0.745(2)	0.664(2)	0.752(7)
	T	1.779(1)	1.620(2)	2.836(2)	1.797(3)

The values for the 3D WB and $b = 3$ MK agrees with those of Ref. [27]

Table 6 Critical exponents of the pure FM fixed point controlling the PM/FM transition for $\pm J$ Ising SG model

	$b = 3$ MK	3D WB	$b = 3$ FC	3D sim. [82]
α	−0.2169(1)	−1.121(1)	−0.1253(1)	0.110(1)
β	1.112(1)	2.282(1)	0.9012(1)	0.3265(3)
γ	−0.006490(1)	−1.443(1)	0.3229(1)	1.2372(5)
δ	0.9942(1)	0.3676(1)	1.358(1)	4.789(2)
ν	0.6850(1)	0.8705(1)	0.6567(1)	0.6301(4)
η	2.009(1)	3.658(1)	1.508(1)	0.0364(5)

Note that $\alpha < 0$ on all HL and, according to the Harris criterion [54], the disorder should be irrelevant. From the analysis of the RG flow this is certainly true for weak disorder. However for large disorder a second, strong disorder, SG fixed point appears controlling the PM/SG transition.

All points on the PM/SG transition line are attracted by the (unstable) SG fixed point located at $p = 0.5$. The $b = 3$ FC HL gives the critical temperature $T_c = 1.072(1)$, with a difference of 4.5 % with respect to the numerical simulation value $T_c = 1.120(4)$ [83]. In

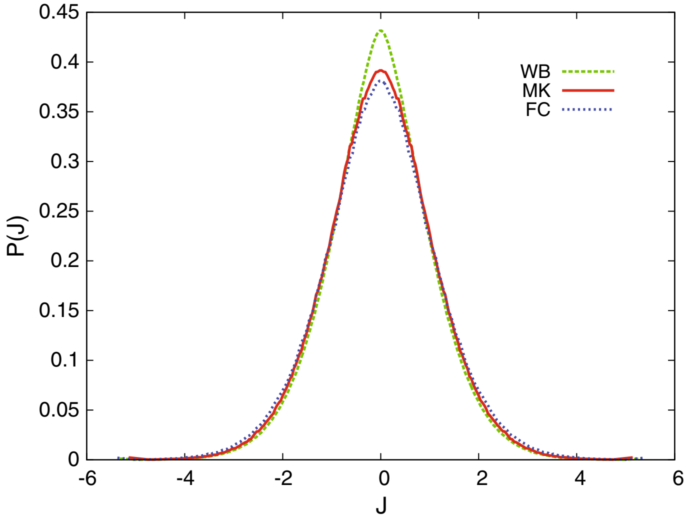

Fig. 12 SG fixed point coupling probability distribution for the $\pm J$ Ising SG model on the $b = 3$ MK lattice (MK), 3D WB HL (WB) and $b = 3$ FC HL (FC).

Table 7 Scaling exponent y_T of the SG fixed point for the $\pm J$ Ising SG model

Lattice	y_T
$b = 3$ MK	0.297 ± 0.026
3D WB	0.308 ± 0.063
$b = 3$ FC	0.262 ± 0.037
3D sim. [84]	0.408 ± 0.025

this case the closest value is obtained with the 3D WB HL, $T_c = 1.112(2)$. The SG fixed point coupling probability distributions P^* is shown in Fig. 12.

The critical exponents can be obtained from the scaling exponents of the SG fixed point evaluated from the RG flow by using the same procedure described for the RFIM, with the simplification of $y = 0$ because the fix point is at finite temperature [49].

The evaluation of y_h is particularly simple. At the SG fixed point $h = h^\dagger = 0$ and $\mathcal{H}^*(-\mathbf{s}) = \mathcal{H}^*(\mathbf{s})$. A straightforward calculation then shows that $\partial h_R/\partial h = c$, the number of links connecting each external sites of the cells with the internal sites. The $b = 3$ FC, 3D WB and MK cell all have $c = b^2$, so that $y_h = 2$.

The scaling exponent y_T is evaluated with the two-pools method measuring $t = \sigma_J - \sigma_J^*$, where σ_J^* is the width of the critical coupling probability distribution P^*. The value of y_T for the different lattices is reported in Table 7. The values are compatible with each other, but quite far from the value $y_T = 0.408 \pm 0.025$ obtained with numerical simulation of the $3D$ lattice. Moreover the worst estimation comes from the $b = 3$ FC HL, a fact enlightening the limitations of the RG approach on HL for the study of the critical properties of disordered systems. The values of the critical exponents are reported in Table 8.

Finally, the stiffness exponent of the SG fixed point is estimated from the growth of σ_J under successive RSRG steps. We find $\theta = 0.2052(1)$, a value remarkably close to what found from numerical simulations: $\theta = 0.19(1)$ [74] or $\theta = 0.20(5)$ [85]. The 3D WB HL

Table 8 Critical exponents of the SG fixed point controlling the PM/SG transition for $\pm J$ Ising SG model

	$b = 3$ MK	3D WB	$b = 3$ FC	3D sim. [84]
α	$-8.10(88)$	$-9.6(24)$	$-10.4(17)$	$-5.4(5)$
β	3.37(30)	4.20(86)	4.27(60)	0.77(5)
γ	3.37(30)	1.35(28)	2.92(41)	5.8(4)
ν	3.37(30)	3.25(66)	3.82(54)	2.45(15)
η	1	1.585 ...	1.236 ...	$-0.375(10)$

The exponent η is equal to $d - 2$, with d the fractal dimension of the HL

leads to $\theta = 0.297(3)$ [27], while the $b = 3$ MK lattice gives $\theta \approx 0.27$ [85], values not as good as the one given by $b = 3$ FC HL.

To summarize, the $b = 3$ FC HL leads to a general improvement in the description of the PM/FM critical behavior, yet the numerical agreement with the numerical simulations is not achieved. A similar general improvement is not seen for the PM/SG critical behavior. In particular the critical exponent ν is badly estimated. The stiffness exponent is, however, very close to the known results from the numerical simulations. We can argue that this follows because the stiffness exponent depends more on the local geometrical properties of the lattice, whose description is improved by the $b = 3$ FC cell, while the critical properties depend on longer distances, still dominated by the hierarchical backbone and thus far from the Bravais lattice behavior.

3 Blume–Emery–Griffiths Model

We now move on to a different system, the Blume–Emery–Griffiths (BEG) model, introduced to study the superfluid transition in He^3–He^4 mixtures [86]. This is a spin-1 model with $s = \pm 1$ representing the magnetic (He^3) sites and $s = 0$ the neutral or hole sites (He^4). The model presents a rich phase diagram with, besides a second order phase transition, a first order transition between the PM and FM phases, in the ordered case, or between the PM and SG phases, in the disordered case.

The ordered model has been studied in both mean-field approximation [86–88] and finite dimension using series extrapolation [89], RSRG analysis [17], Monte Carlo simulations [90], effective-field theory [91] or two-particle cluster approximation [92].

The inclusion of weak and strong quenched disorder has been studied in the mean-field limit [36,38,93,94], finite dimensional RSRG analysis on MK lattices [33,95] and Monte Carlo simulations [37,39,40,96].

The numerical simulation shows that also in the disordered case, and similar to what predicted by the mean-field analysis, the second order transition line ends at a tricritical point where a first order transition develops. For positive and finite values of the chemical potential of the holes the first order transition line bends leading to the so called *inverse freezing* phenomenon, i.e., the arrest of the amorphous phase in a solid-like state upon heating [37,38]. Contrarily to these findings, the RSRG study of the disordered model on MK lattices does not reveal this first order phase transition, nor the reentrance of the transition line [33].

In this section we deepen the RSRG study of the disorder BEG model by comparing the results on the $b = 3$ MK lattice (Fig. 10), the $b = 2$ MK lattice (Fig. 13), the 3D WB HL (Fig. 3) and the $b = 3$ FC HL (Fig. 9).

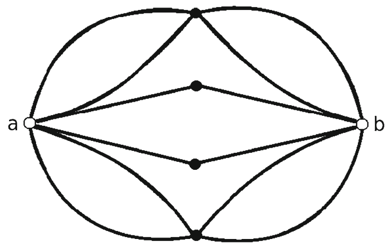

Fig. 13 $b = 2$ MK cell with fractal dimension $d = 3.58$, the same of the 3D WB cell, cfr. Fig. 3

The form of the BEG Hamiltonian suitable for the RG study is

$$-\beta\mathcal{H}(\boldsymbol{s}) = \sum_{\langle ij\rangle} J_{ij} s_i s_j + \sum_{\langle ij\rangle} K_{ij} s_i^2 s_j^2 - \sum_{\langle ij\rangle} \Delta_{ij}\left(s_i^2 + s_j^2\right) - \sum_{\langle ij\rangle} \Delta_{ij}^{\dagger}\left(s_i^2 - s_j^2\right) \tag{14}$$

where $s_i = \pm 1, 0$ and, in the strong disordered case,

$$P(\mathcal{K}_{ij}) = \frac{1}{2}\Big[\delta(J_{ij} - J) + \delta(J_{ij} + J)\Big]\,\delta(K_{ij})\,\delta(\Delta_{ij} - \Delta)\,\delta\left(\Delta_{ij}^{\dagger}\right), \tag{15}$$

with $\mathcal{K}_{ij} = (J_{ij}, K_{ij}, \Delta_{ij}, \Delta_{ij}^{\dagger})$. In the limit $\Delta \ll -1$ the values $s_i = 0$ are suppressed and the model goes over the $\pm J$ Ising SG model discussed in the previous section with $p = 1/2$.

For any given coupling configuration the RG equation $\boldsymbol{\mathcal{K}}^R = \mathcal{R}(\boldsymbol{\mathcal{K}})$ generated by the block RG transform on the cell $\mathcal{C}_{ab}$ are

$$\begin{aligned} J_R &= \frac{1}{2}\log\left(\frac{x_{++}}{x_{+-}}\right), & K_R &= \frac{1}{2}\log\left(\frac{x_{++}\,x_{+-}\,x_{00}^2}{x_{0+}^2\,x_{+0}^2}\right), \\ \Delta_R &= \frac{1}{2}\log\left(\frac{x_{00}^2}{x_{+0}\,x_{0+}}\right), & \Delta_R^{\dagger} &= \frac{1}{2}\log\left(\frac{x_{+0}}{x_{0+}}\right), \end{aligned} \tag{16}$$

where $x_{s_a s_b}$ are the edge Boltzmann factors, Eq. (2).

The phase diagram obtained with the different lattices is shown in Fig. 14. The projection of the renormalized $P(\mathcal{K})$ is plotted in Fig. 15. In all cases the PM/SG transition is second order. All points on the critical PM/SG surface flow under RG towards the Ising SG fixed point at $\mu_\Delta \to -\infty$, $\sigma_\Delta \to 0$. The PM/SG transition is then in the same universality class of the PM/SG transition in the Ising SG model discussed in the previous section.

We have no clear evidence on why the first order transition is missing. Based on physical arguments we may propose the following conjecture. A second order transition is associated with an instability, the high temperature phase becomes unstable and a new stable phase appears continuously. The instability can manifest itself locally, and hence HL can capture second order transitions. A first order transitions, on the contrary, is not triggered by an instability. The high temperature phase remains stable, but a thermodynamically more favorable phase takes over. Such a situation requires some sort of long range structure of the lattice, structure that is missing in the HL we have considered, and this explains why we do not see the first order transition. If our conjecture is correct one may wonder if the first order transition could appear on HL with folded cells with large but finite b. The drawback is that the value of b could be so large to make the whole HL approach ineffective. The analysis on this direction is left for future work.

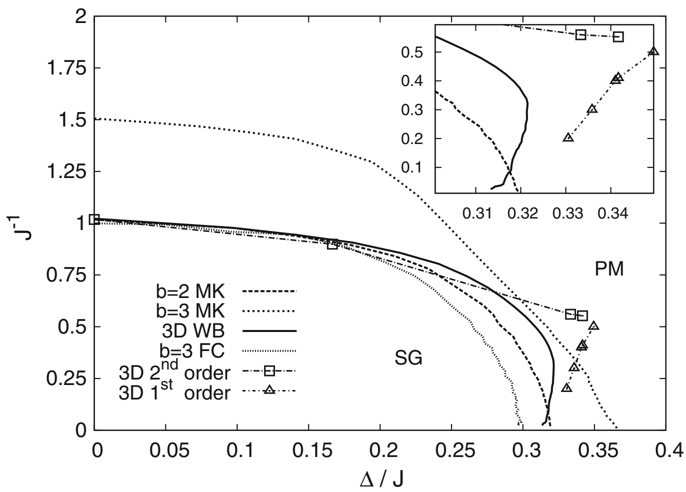

Fig. 14 RSRG phase diagram of the disordered BEG model compared with the result from numerical simulation on 3D lattice (3D) [37] *Inset* detail of the reentrance seen on the 3D WB HL and absent on MK lattices

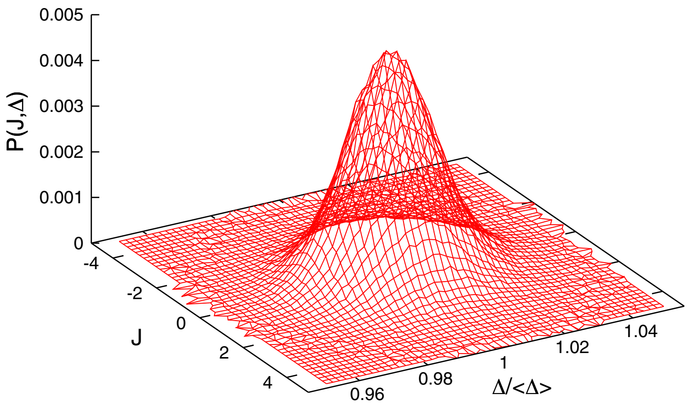

Fig. 15 Projection of Ising SG fixed point probability distribution $P^*(\mathcal{K})$ for the disordered BEG model on the $b = 3$ WB HL. The results with the MK lattices and $b = 3$ FC HL are similar

The re-entrance of the transition line, unseen with MK lattices, is however found, but only with the 3D WB HL.

4 Discussion

The RSRG on hierarchical lattices is a simple and powerful method for studying the critical behavior of model systems, much faster than Monte Carlo simulations on Bravais lattices. Despite the numerical outcomes usually differ from those on Bravais lattices, it can provide information on the general features of the critical behavior. The method, however, presents some drawbacks and the picture that emerges may lack some important aspects.

In this work we have provided a critical analysis of the RSRG on MK and more structured hierarchical lattices by studying the critical behavior of the RFIM, the Random Bond Ising Model and the Blume–Emery–Griffiths. The models have been chosen as representative of some typical behaviors: ferromagnetic, AFM and spin-glass phases, first and second order transitions.

Our results provide a clue to the possibility of obtaining approximations of models on regular lattice by similar models on hierarchical lattice. We show that it is possible to obtain a good picture of the actual phase diagram, but far more difficult to yield a proper determination of critical exponents.

By introducing more structured elementary cells one hopes of capturing the local geometrical properties of the bonds. At least part of it. For pure models, although it is not a systematic approximation, a general improvement is obtained using unit cells that locally mimic better the connectivity of the Bravais lattice. In the disordered case, instead, the situation is less definite, and no net improvement is observed: the 3D WB cell (Fig. 3) proves to be the slightly most reliable, generally quantitatively better than the more complex FC of Fig. 9. In particular, it shows the expected inverse transition for the BEG model, but we cannot give a general explanation for this.

The fractal dimension of the lattice seems to play a minor role, as the three dimensional regular lattice is better approximated by the 3D WB with $d = 3.58\ldots$, compared to the $b = 3$ MK with $d = 3$ (Fig. 10) and the $b = 3$ FC (Fig. 9) with $d = 3.24\ldots$, while the $b = 2$ MK (Fig. 13) with $d = 3.58\ldots$ gives the worst approximation by far.

The scaling factor b has the known role to determine if the AFM order can be preserved, as it is possible only when b is odd so that negative interactions in the unit cell involve negative interactions between the external sites, and the phase diagram turns out symmetric under the inversion of the bonds sign. Our results indicate that this feature does not play a crucial role in the disordered systems, at least until the negative bonds become dominant. The two investigated hierarchical lattices with even b, the 3D WB and the $b = 2$ MK, indeed, appear to be, respectively, the best and the worst in approximating the phase diagram of the models on regular lattice. The only case in which the $b = 3$ FC lattice provides a remarkable improvement with respect to the 3D WB lattice is in the estimate of the SG stiffness exponent. A more structured inner local connectivity could, thus, become important at low temperatures.

In conclusion, our results show that the RSRG on hierarchical lattices is particularly poor for disordered systems, and strongly suggest that its limitations are intrinsic to the hierarchical nature. The most striking case is the lack of first order transition in the BEG model. Using more structured cells may, indeed, improve the treatment of short distances, i.e., short loops, however the longer distances appear definitely dominated by the hierarchical nature of the lattice.

Finally as byproduct of our analysis, and besides the evaluation of the critical exponents, we have found indications that the bimodal and Gaussian Random Field model in dimension $d < 2.5$ are in the same universality class. Moreover, the Nishimori conjecture appears always violated, whereas the Harris criterion is violated only above dimension 2.5.

Acknowledgments The research leading to these results has received funding from the People Programme (Marie Curie Actions) of the European Union's Seventh Framework Programme FP7/2007-2013/ under REA grant agreement n 290038, NETADIS project and from the Italian MIUR under the Basic Research Investigation Fund FIRB2008 program, Grant No. RBFR08M3P4, and under the PRIN2010 program, grant code 2010HXAW77-008.

References

1. Parisi, G.: Infinite number of order parameters for spin-glasses. Phys. Rev. Lett. **43**, 1754n++1756 (1979)
2. Parisi, G.: A sequence of approximated solutions to the S–K model for spin glasses. J. Phys. A Math. Gen. **13**, L115 (1980)
3. Mézard, M., Parisi, G., Virasoro, M.: Spin Glass Theory and Beyond. World Scientific, Singapore (1987)
4. Amit, D.J.: Modeling Brain Functions: The World of Attractor Neural Networks. Cambridge University Press, Cambridge (1992)
5. Mézard, M., Montanari, A.: Information, Physics, and Computation. Oxford University Press, Oxford (2009)
6. Chen, J.H., Lubensky, T.C.: Mean field and ϵ-expansion study of spin glasses. Phys. Rev. B **16**, 2106 (1977)
7. De Dominicis, C., Kondor, I., Temesvari, T.: Beyond the Sherrington–Kirkpatrick model. In: Directions in Condensed Matter Physics, vol. 12, p. 119. World Scientific, Singapore (1998)
8. De Dominicis, C., Giardina, I.: Random Fields and Spin Glasses. Cambridge University Press, Cambridge (2006)
9. Bray, A.J., Moore, M.A.: Disappearance of the de Almeida-Thouless line in six dimensions. Phys. Rev. B **83**, 224408 (2011)
10. Parisi, G., Temesvari, T.: Replica symmetry breaking in and around six dimensions. Nucl. Phys. B [FS] **858**, 293–316 (2012)
11. Stein, D.L., Newman, C.M.: Spin Glasses and Complexity. Princeton University Press, Princeton (2012)
12. Amit, D.J., Martin-Mayor, V.: Field Theory; The Renormalization Group and Critical Phenomena. World Scientific, Singapore (2005)
13. Le Bellac, M.: Quantum and Statistical Field Theory. Oxford Science Publications, Oxford (1992)
14. Kadanoff, L.P.: Notes on Migdal's recursion formulas. Ann. Phys. **100**(1), 359–394 (1976)
15. Ma, S.K.: Modern Theory of Critical Phenomena. Benjamin-Cummings, Reading (1976)
16. Leeuwen, J.M.J., Niemeijer, T.: Wilson theory for spin systems on triangular lattice. Phys. Rev. Lett. **31**(23), 1411 (1973)
17. Berker, A.N., Wortis, M.: Blume–Emery–Griffiths–Potts model in two dimensions: phase diagram and critical proprieties from a position-space renormalization group. Phys. Rev. B **14**(11), 4946 (1976)
18. Fisher, K.H., Kinzel, W.: Existence of a phase transition in spin glasses? J. Phys. C **11**, 2115 (1978)
19. Tatsumi, T.: Renormalization-group approach to spin glass transition of a random bond Ising model in two- and three-dimensions. Prog. Theor. Phys. **59**, 405 (1978)
20. Franz, S., Parisi, G., Virasoro, M.A.: Interfaces and louver critical dimension in a spin glass model. J. Phys. I (France) **4**, 1657 (1994)
21. Franz, S., Toninelli, F.L.: A field-theoretical approach to the spin glass transition: models with long but finite interaction range. J. Stat. Mech. P01008 (2005)
22. Boettcher, S.: Stiffness of the Edwards–Anderson model in all dimensions. Phys. Rev. Lett. **95**, 197205 (2005)
23. Berker, A.N., Ostlund, S.: Renormalisation-group calculations of finite systems: order parameter and specific heat for epitaxial ordering. J. Phys. C **12**(22), 4961 (1979)
24. Griffiths, R.B., Kaufman, M.: Spin systems on hierarchical lattices. Introduction and thermodynamic limit. Phys. Rev. B **26**, 5022–5032 (1982)
25. McKay, S.R., Berker, A.N., Kirkpatrick, S.: Spin-glass behavior in frustrated Ising models with chaotic renormalization-group trajectories. Phys. Rev. Lett. **48**, 767–770 (1982)
26. Ohzeki, M., Nishimori, H., Berker, A.N.: Multicritical points for spin-glass models on hierarchical lattices. Phys. Rev. E **77**, 061116 (2008)
27. Salmon, O.R., Agostini, B.T., Nobre, F.D.: Ising spin glasses on Wheatstone–Bridge hierarchical lattices. Phys. Lett. A **374**(15–16), 1631–1635 (2010)
28. Moore, M.A., Bokil, H., Drossel, B.: Evidence for the droplet picture of spin glasses. Phys. Rev. Lett. **81**, 4252 (1998)
29. Ricci-Tersenghi, F., Ritort, F.: Absence of ageing in the remanent magnetization in Migdal–Kadanoff spin glasses. J. Phys. A Math. Gen. **33**, 3727 (2000)
30. Nobre, F.D.: Phase diagram of the two-dimensional ±J Ising spin glass. Phys. Rev. E **64**, 046108 (2001)
31. Nishimori, H., Ohzeki, M.: Multicritical point of spin glasses. Phys. A Stat. Mech. Appl. **389**, 2907–2910 (2010)
32. Andelman, D., Berker, A.N.: q-State Potts models in *d* dimensions: Migdal–Kadanoff approximation. J. Phys. A Math. Gen. **14**(4), L91 (1981)
33. Ozcelik, V.O., Berker, A.N.: Blume–Emery–Griffiths spin glass and inverted tricritical points. Phys. Rev. E **78**, 031104 (2008)

34. da Silva, L.R., Tsallis, C., Schwachheim, G.: Anisotropic cubic lattice Potts ferromagnet: renormalisation group treatment. J. Phys. A Math. Gen. **17**, 3209 (1984)
35. Tsallis, C., de Magalhães, A.C.N.: Pure and random Potts-like models: real-space renormalization-group approach. Phys. Rep. **268**(5–6), 305–430 (1996)
36. Crisanti, A., Leuzzi, L.: Stable solution of the simplest spin model for inverse freezing. Phys. Rev. Lett. **95**, 087201 (2005)
37. Paoluzzi, M., Leuzzi, L., Crisanti, A.: Thermodynamic first order transition and inverse freezing in a 3D spin glass. Phys. Rev. Lett. **104**, 120602 (2010)
38. Crisanti, A., Leuzzi, L., Rizzo, T.: Complexity in mean-field spin glass models: the Ising p-spin. Phys. Rev. B **71**, 094202 (2005)
39. Leuzzi, L., Paoluzzi, M., Crisanti, A.: Random Blume–Capel model on a cubic lattice: first-order inverse freezing in a three-dimensional spin-glass system. Phys. Rev. B **83**, 014107 (2011)
40. Paoluzzi, M., Leuzzi, L., Crisanti, A.: The overlap parameter across an inverse first-order phase transition in a 3D spin-glass. Philos. Mag. **91**, 1966–1976 (2011)
41. Migdal, A.A.: Phase transitions in gauge and spin-lattice systems. Zh. Eksp. Teor. Fiz. **69**, 1457 (1975)
42. Cardy, J.: Scaling and Renormalization in Statistical Physics. Cambridge Lecture Notes in Physics. Cambridge University Press, Cambridge (1996)
43. Harris, A.B., Lubemsky, T.C.: Renormalization-group approach to the critical behavior of random-spin models. Phys. Rev. Lett. **33**, 1540 (1974)
44. Andelman, D., Berker, A.N.: Scale-invariant quenched disorder and its stability criterion at random critical points. Phys. Rev. B **29**, 2630–2635 (1984)
45. Southern, B.W., Young, A.P.: Real space rescaling study of spin glass behaviour in three dimensions. J. Phys. C **10**, 2179 (1977)
46. Cao, M.S., Machta, J.: Migdal-Kadanoff study of the random-field Ising model. Phys. Rev. B **48**, 3177–3182 (1993)
47. Salmon, O.R., Nobre, F.D.: Spin-glass attractor on tridimensional hierarchical lattices in the presence of an external magnetic field. Phys. Rev. E **79**, 051122 (2009)
48. Berker, A.N.: Comment on "Spin-glass attractor on tridimensional hierarchical lattices in the presence of an external magnetic field". Phys. Rev. E **81**, 043101 (2010)
49. Bray, A.J., Moore, M.A.: Scaling theory of the random-field Ising model. J. Phys. C. Solid State Phys. **18**(28), L927 (1985)
50. Berker, A.N., McKay, S.R.: Modified hyperscaling relation for phase transitions under random fields. Phys. Rev. B **33**, 4712–4715 (1986)
51. Falicov, A., Berker, A.N., McKay, S.R.: Renormalization-group theory of the random-field Ising model in three dimensions. Phys. Rev. B **51**, 8266–8269 (1995)
52. Middleton, A.A., Fisher, D.S.: Three-dimensional random-field Ising magnet: interfaces, scaling, and the nature of states. Phys. Rev. B **65**, 134411 (2002)
53. Hartmann, A.K.: Critical exponents of four-dimensional random-field Ising systems. Phys. Rev. B **65**, 174427 (2002)
54. Harris, A.B.: Effect of random defects on the critical behaviour of Ising models. J. Phys. C Solid State Phys. **7**, 1671 (1974)
55. Chayes, J.T., Chayes, L., Fisher, D.S., Spencer, T.: Finite-size scaling and correlation lengths for disordered systems. Phys. Rev. Lett. **57**, 2999–3002 (1986)
56. Kinzel, W., Domany, E.: Critical properties of random Potts models. Phys. Rev. B **23**, 3421–3434 (1981)
57. Andelman, D., Aharony, A.: Critical behavior with axially correlated random bonds. Phys. Rev. B **31**, 4305–4312 (1985)
58. Derrida, B., Dickinson, H., Yeomans, J.: On the Harris criterion for hierarchical lattices. J. Phys. A **18**(1), L53 (1985)
59. Mukherji, S., Bhattacharjee, S.M.: Failure of the Harris criterion for directed polymers on hierarchical lattices. Phys. Rev. E **52**, 1930–1933 (1995)
60. Efrat, A.: Harris criterion on hierarchical lattices: rigorous inequalities and counterexamples in Ising systems. Phys. Rev. E **63**, 066112 (2001)
61. Domany, E.: Some results for the two-dimensional Ising model with competing interactions. J. Phys. C **12**, L119 (1979)
62. Ohzeki, M., Thomas, C.K., Katzgraber, H.G., Bombin, H., Martin-Delgado, M.A.: Lack of universality in phase boundary slopes for spin glasses on self dual lattices. J. Stat. Mech. P02004 (2011)
63. Ohzeki, M., Nishimori, H.: Analytical evidence for the absence of spin glass transition on self-dual lattices. J. Phys. A Math. Gen. **42**, 332001 (2009)
64. Nishimori, H.: Internal energy, specific heat and correlation function of the bond-random Ising model. Prog. Theor. Phys. **66**, 1169 (1981)

65. Nishimori, H.: Statistical Physics of Spin Glasses and Information Processing: An Introduction. Oxford University Press, Oxford (2001)
66. Nishimori, H., Nemoto, K.: Duality and multicritical point of two-dimensional spin glasses. J. Phys. Soc. Jpn. **71**, 1198 (2002)
67. Maillard, J.M., Nemoto, K., Nishimori, H.: Symmetry, complexity and multicritical point of the two-dimensional spin glass. J. Phys. A **36**, 9799 (2003)
68. Takeda, K., Nishimori, H.: Self-dual random-plaquette gauge model and the quantum toric code. Nucl. Phys. B **686**(3), 377–396 (2004)
69. Hinczewski, M., Berker, A.N.: Multicritical point relations in three dual pairs of hierarchical-lattice Ising spin glasses. Phys. Rev. B **72**, 144402 (2005)
70. Reis, F.D.A.A., de Queiroz, S.L.A., dos Santos, R.R.: Universality, frustration, and conformal invariance in two-dimensional random Ising magnets. Phys. Rev. B **60**, 6740–6748 (1999)
71. Singh, R.R.P., Adler, J.: High-temperature expansion study of the Nishimori multicritical point in two and four dimensions. Phys. Rev. B **54**, 364–367 (1996)
72. Ozeki, Y., Ito, N.: Multicritical dynamics for the +/− J Ising model. J. Phys. A **31**, 5451 (1998)
73. Kawashima, N., Rieger, H.: Finite-size scaling analysis of exact ground states for +/−J spin glass models in two dimensions. Europhys. Lett. **39**, 85 (1997)
74. Bray, A.J., Moore, M.A.: Heidelberg colloquium on glassy dynamics. In: van Hemmen, J.L. (ed) Lecture Notes in Physics., vol. 275, pp. 121–153. Springer, Berlin (1987)
75. Bray, A.J., Moore, M.A.: Lower critical dimension of Ising spin glasses: a numerical study. J. Phys. C **17**(18), L463 (1984)
76. Nobre, F.D.: Real-space renormalization-group approaches for two-dimensional Gaussian Ising spin glass. Phys. Lett. A **250**, 163 (1998)
77. Hartmann, A.K., Bray, A.J., Carter, A.C., Moore, M.A., Young, A.P.: Stiffness exponent of two-dimensional Ising spin glasses for nonperiodic boundary conditions using aspect-ratio scaling. Phys. Rev. B **66**, 224401 (2002)
78. Weigel, M., Johnston, D.: Frustration effects in antiferromagnets on planar random graphs. Phys. Rev. B **76**, 054408 (2007)
79. Erbas, A., Tuncer, A., Yücesoy, B., Berker, A.N.: Phase diagrams and crossover in spatially anisotropic $d = 3$ Ising, XY magnetic, and percolation systems: exact renormalization-group solutions of hierarchical models. Phys. Rev. E **72**, 026129 (2005)
80. Talapov, A.L., Blöte, H.W.J.: The magnetization of the 3D Ising model. J. Phys. A **29**(17), 5727 (1996)
81. Nienhuis, B., Nauenberg, M.: First-order phase transitions in renormalization-group theory. Phys. Rev. Lett. **35**, 477–479 (1975)
82. Pelissetto, A., Vicari, E.: Critical phenomena and renormalization-group theory. Phys. Rep. **368**, 549–727 (2002)
83. Katzgraber, H.G., Körner, M., Young, A.P.: Universality in three-dimensional Ising spin glasses: a Monte Carlo study. Phys. Rev. B **73**(22), 224432 (2006)
84. Hasenbusch, M., Pelissetto, A., Vicari, E.: Critical behavior of three-dimensional Ising spin glass models. Phys. Rev. B **78**, 214205 (2008)
85. Jörg, T., Katzgraber, H.G.: Evidence for universal scaling in the spin-glass phase. Phys. Rev. Lett. **101**(19), 197205 (2008)
86. Blume, M., Emery, V.J., Griffiths, R.B.: Ising model for the λ transition and phase separation in He^3–He^4 mixtures. Phys. Rev. A **4**, 1071–1077 (1971)
87. Blume, M.: Theory of the first-order magnetic phase change in UO_2. Phys. Rev. **141**, 517 (1966)
88. Capel, H.W.: On the possibility of first-order phase transitions in Ising systems of triplet ions with zero-field splitting. Physica **32**, 966 (1966)
89. Saul, D.M., Wortis, M., Stauffer, D.: Tricritical behavior of the Blume–Capel model. Phys. Rev. B **9**, 4964 (1974)
90. Deserno, M.: Tricriticality and the Blume–Capel model: a Monte Carlo study within the microcanonical ensemble. Phys. Rev. E **56**, 5204 (1997)
91. Chakraborty, K.G.: Effective-field model for a spin-1 Ising system with dipolar and quadrupolar interactions. Phys. Rev. B **29**, 1454–1457 (1984)
92. Baran, O.R., Levitskii, R.R.: Reentrant phase transitions in the Blume–Emery–Griffiths model on a simple cubic lattice: the two-particle cluster approximation. Phys. Rev. B **65**, 172407 (2002)
93. Crisanti, A., Leuzzi, L.: First-order phase transition and phase coexistence in a spin-glass model. Phys. Rev. Lett. **89**, 237204 (2002)
94. Crisanti, A., Ritort, F.: Intermittency of glassy relaxation and the emergence of a non-equilibirum spontaneous measure in the aging regime. Europhys. Lett. **66**, 253 (2004)

95. Falicov, A., Berker, A.N.: Tricritical and critical end-point phenomena under random bonds. Phys. Rev. Lett. **76**, 4380–4383 (1996)
96. Puha, I., Diep, H.T.: Random-bond and random-anisotropy effects in the phase diagram of the Blume–Capel model. J. Magn. Magn. Mater. **224**, 85–92 (2000)